



HAL
open science

CENTRAL SEROUS CHORIORETINOPATHY High-Resolution Imaging of Asymptomatic Fellow Eyes Using Adaptive Optics Scanning Laser Ophthalmoscopy

Melvin Gerardy, Nilufer Yesilirmak, Richard Legras, Francine Behar-Cohen,
Elodie Bousquet, ‡ Elodie Bousquet

► **To cite this version:**

Melvin Gerardy, Nilufer Yesilirmak, Richard Legras, Francine Behar-Cohen, Elodie Bousquet, et al..
CENTRAL SEROUS CHORIORETINOPATHY High-Resolution Imaging of Asymptomatic Fellow
Eyes Using Adaptive Optics Scanning Laser Ophthalmoscopy. *RETINA. The Journal of Retinal and
Vitreous Diseases*, 2022, 42 (2), pp.375-380. 10.1097/IAE.0000000000003311 . hal-03549577

HAL Id: hal-03549577

<https://hal.sorbonne-universite.fr/hal-03549577v1>

Submitted on 31 Jan 2022

HAL is a multi-disciplinary open access archive for the deposit and dissemination of scientific research documents, whether they are published or not. The documents may come from teaching and research institutions in France or abroad, or from public or private research centers.

L'archive ouverte pluridisciplinaire **HAL**, est destinée au dépôt et à la diffusion de documents scientifiques de niveau recherche, publiés ou non, émanant des établissements d'enseignement et de recherche français ou étrangers, des laboratoires publics ou privés.

CENTRAL SEROUS CHORIORETINOPATHY

High-Resolution Imaging of Asymptomatic Fellow Eyes Using Adaptive Optics Scanning Laser Ophthalmoscopy

MELVIN GERARDY, MD,* NILUFER YESILIRMAK, MD,* RICHARD LEGRAS, PhD,†
FRANCINE BEHAR-COHEN, MD, PhD,*‡ ELODIE BOUSQUET, MD, PhD*‡

Purpose: To investigate cone density in the asymptomatic fellow eye of patients with unilateral central serous chorioretinopathy (CSCR).

Methods: Seventeen asymptomatic fellow eyes of patients with unilateral CSCR and 17 eyes of aged-matched and gender-matched healthy controls underwent adaptive optics ophthalmoscopy. Cone density and spacing were assessed at the fovea. Clinical and multimodal imaging findings were also recorded.

Results: In the CSCR group, the patient mean age was 48.9 ± 9.8 years. The mean (\pm SD) subfoveal choroidal thickness was $417.8 \pm 125.2 \mu\text{m}$. The foveal external limiting membrane and ellipsoid zone were intact in all patients. Adaptive optics fundus imaging showed a significant decrease in cone density at 2° of eccentricity nasal and temporal to the fovea in asymptomatic fellow eyes of patients with unilateral CSCR compared with controls ($P = 0.001$ and $P = 0.027$, respectively). No statistically significant difference in cone density was found at 4° of eccentricity nasal and temporal to the fovea between both groups.

Conclusion: Asymptomatic fellow eyes of patients with unilateral CSCR showed a reduced density of foveal cones in the absence of a decreased visual acuity and photoreceptor line disruption on optical coherence tomography. These results suggest that the photoreceptors could be damaged independently of the occurrence of a serous retinal detachment.

RETINA 42:375–380, 2022

Central serous chorioretinopathy (CSCR) is characterized by the presence of a serous retinal detachment (SRD) associated with retinal pigment epithelium (RPE) alterations and increased choroidal thickness.¹ Central serous chorioretinopathy shows features of the pachychoroid disease phenotype that is characterized by the presence of dilated choroidal vessels in the Haller layer, associated with a thinning of the choriocapillaris and Sattler layer called pachyvessels.² Other diseases related to these pachychoroid features have been reported, including pachychoroid pigment epitheliopathy (PPE), pachychoroid neovasculopathy, polypoidal choroidal vasculopathy, and peripapillary pachychoroid syndrome.² Whether these entities are the progressive evolution of a single entity or a singular clinical manifestation complicating an underlying pachychoroid phenotype is a matter of debate.³

The term “PPE” was first introduced by Warrow et al⁴ to describe RPE changes occurring in areas of choroidal

thickening in patients without a history or clinical signs of previous subretinal detachment. Although acute CSCR is unilateral on presentation, in most cases, about half of the patients experience PPE in their asymptomatic fellow eye.^{5,6} In addition, a thinning of the outer nuclear layer has also been described in eyes with PPE, possibly related to focal choroidal ischemia and subsequent RPE disruption and photoreceptor apoptosis.⁷ These observations suggest that RPE and outer retinal alterations may develop in the absence of subretinal fluid and result from a dysregulation of the choroidal blood flow.

Adaptive optics (AO) retinal imaging, which uses movable mirrors to compensate for aberrations in the optical path between the retina and the camera, allows visualizing in vivo individual cone photoreceptors.⁸ However, cone imaging is impaired when a subretinal fluid or retinal pigment epithelium detachment is present, limiting its potential in patients with active

CSCR. In the two published studies that have assessed CSCR eyes,^{9,10} the photoreceptor mosaic changes have thus been assessed in patients with resolved subretinal fluid and a lower cone density has been shown compared with normal healthy eyes and interpreted as a consequence of the SRD. However, whether cone photoreceptors could be altered in the asymptomatic fellow eye of patients with unilateral CSCR in the absence of any subretinal fluid remains unknown.

The aim of this study was to investigate cone density in the asymptomatic fellow eyes of patients with unilateral CSCR by AO imaging and to compare it with that found in healthy age-matched and gender-matched eyes.

Materials and Methods

Study Design

This was a monocentric, observational, retrospective study conducted in a tertiary ophthalmologic center, Ophtalmopôle, Cochin Hospital, Paris, between June 2018 and April 2019.

Ethics Statement

The study protocol adhered to the tenets of the Declaration of Helsinki and was approved by the Ethics Committee of the French Society of Ophthalmology (IRB 00008855 from Société Française d'Ophtalmologie). Informed consent was obtained before performing the imaging procedures from each patient and healthy subject.

Study Patients

Data on the asymptomatic fellow eyes of patients with unilateral CSCR imaged with AO fundus imaging were analyzed. Only fellow eyes with 20/20 visual acuity and without detectable signs of previous SRD were included

in the study. The exclusion criteria were (1) fellow eyes with ongoing SRD, or with a previous history of SRD, confirmed by OCT and/or blue-light fundus autofluorescence (BAF); (2) fellow eyes with pigment epithelium detachment (PED) or bulges/irregularities in the macular area; (3) patients with other retinal diseases, including high myopia or hypermetropia (>-6 diopters or $<+6$ diopters); and (4) insufficient pharmacologically induced mydriasis (<5 mm).

These fellow eyes without any history of previous CSCR episode and without any symptoms or signs of SRD were considered as unaffected contralateral eyes and referred in the article as “asymptomatic fellow eye.” The eye with CSCR was referred as “active CSCR eye.”

In addition, a group of age-matched and gender-matched patients without ocular disease and with normal fundus examination and normal macular OCT was used as a control group.

Study Protocol and Imaging Analysis

The medical and imaging data collected included age, sex, history of corticosteroid intake, the best-corrected visual acuity (BCVA) converted into log-MAR scale, spectral domain OCT with enhanced depth imaging (EDI) mode (Heidelberg Spectralis; Heidelberg, Germany), BAF, and fluorescein (FA) and indocyanine green angiography (Spectralis). The clinical form of the disease in the active CSCR eye was also recorded. Chronic CSCR was defined by the presence of a persistent SRD for at least 6 months. In other cases, CSCR was classified as acute/recurrent. The choroidal thickness was manually measured on EDI horizontal B-scans passing through the fovea. The presence of a PED or bulges/irregularities on the SD-OCT B-scan was recorded. The integrity of the foveal external limiting membrane and ellipsoid zone was assessed by spectral domain-optical coherence tomography and classified into two categories: intact or fragmented/absent by two trained retina specialists (M.G. and E.B.). Disagreements were resolved by an open adjudication. Blue-light autofluorescence images were assessed to confirm the presence of hyperautofluorescent or hypoautofluorescent areas corresponding to RPE alterations. On indocyanine green angiography, the presence of dilated choroidal veins (pachyvessels) in the early phase and the presence of hyperpermeability plaques in the midphase were recorded.

Adaptive Optics Fundus Imaging Acquisition and Analysis

Patients underwent AO fundus imaging (rtx1; Imagine Eyes, Orsay, France). The imaging field size of this commercial clinical prototype is $4^\circ \times 4^\circ$, which is

From the *Department of Ophthalmology, Ophtalmopôle, Hôpital Cochin, Assistance Publique-Hôpitaux de Paris, AP-HP, Université de Paris, Paris, France; †Laboratoire Lumière, Matière et Interfaces, CNRS, ENS Paris-Saclay, Centrale Supélec, Université Paris Saclay, Orsay, France; and ‡Centre de Recherche des Cordeliers, INSERM U1138, Physiopathology of Ocular Diseases: Therapeutic Innovations, Université de Paris, Paris, France.

This study was supported by the Katz family foundation.

None of the authors has no conflicting interests to disclose.

This is an open access article distributed under the terms of the Creative Commons Attribution-Non Commercial-No Derivatives License 4.0 (CCBY-NC-ND), where it is permissible to download and share the work provided it is properly cited. The work cannot be changed in any way or used commercially without permission from the journal.

Reprint requests: Francine Behar-Cohen, MD, PhD, Department of Ophthalmology, Ophtalmopôle, Hôpital Cochin, Assistance Publique-Hôpitaux de Paris, AP-HP, Université de Paris, 8 Rue Méchain, 75014 Paris, France; e-mail: francine.behar@gmail.com

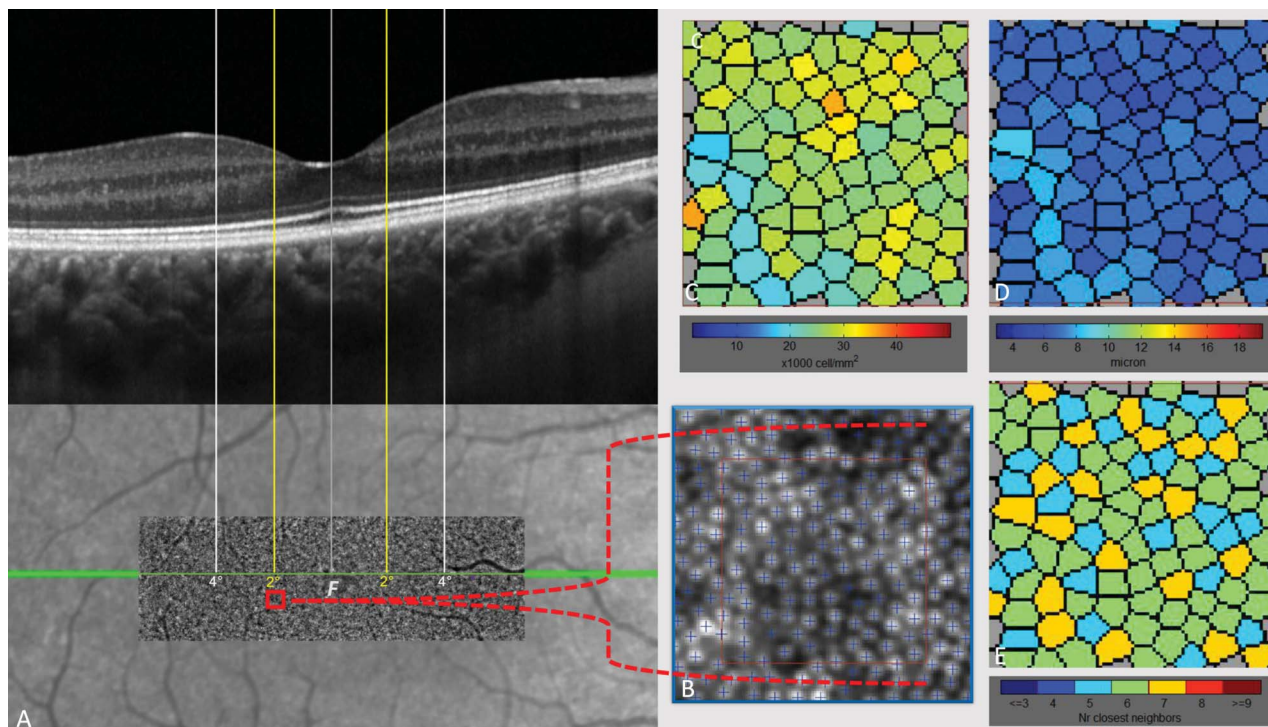


FIGURE 1. Adaptive optics retinal imaging of the asymptomatic fellow eye of a 40-year-old woman with unilateral chronic central serous chorioretinopathy. **A.** Colocation of the AO montage with the corresponding OCT B-scan centered on the fovea (the green line indicates the position of the OCT B-scan) and with the laser scanner optics to determine the exact position of the fovea and the retinal eccentricities at 2° and 4° nasal and temporal to the fovea. Cones in the very center of the fovea appear blurred because of the resolution limit of the AO camera. **B.** Magnified image of the sampling window of 50 $\mu\text{m} \times 50 \mu\text{m}$ at 2° of eccentricity temporal to the fovea with cone counted using automated AO detect software. **C.** Density map of the corresponding cone count sampling window. **D.** Interphotoreceptor distance map of the corresponding cone count sampling window. **E.** Packing regularity of the corresponding cone count sampling window representing the number of the nearest neighboring cones.

equivalent to 1.2 mm \times 1.2 mm on the retina. Retinal images were acquired at 0°, 2°, 4°, and 6° of eccentricity, along the four meridians (nasal, temporal, superior, and inferior), with the patient fixating on a cross controlled by the operator during the examination. The imaging depth was chosen to have the sharpest live retina images. Foveolar cone densities (inside a circle of <2° of radius) cannot be imaged using the rtx1 AO device because of the small size and packed arrangements of the central foveal cones¹¹ and limitations in the system wavefront compensation capabilities.¹²

For one final image, a set of 40 raw images of the same retinal area were acquired automatically at a rate of 9.5 frames per second with an exposure time of 10 ms. These images were recorded and averaged to display a final image with an improved signal-to-noise ratio^{13,14} (Figure 1). The test–retest variability of rtx1 and its software was shown to be good in a previous study.¹⁵

AO Image Analyzes

Adaptive optics images of adjacent retinal areas along the horizontal meridian were mounted together

to obtain a montage covering up to $\pm 6^\circ$ of eccentricity from the foveal center using i2k software (DualAlign, Clifton Park, NY). Each montage was aligned with the SLO-IR and OCT images acquired in the same eye using PowerPoint software (Microsoft, Seattle, WA). The foveal center of the montage images was determined as previously described.¹²

Cones along the horizontal meridian corresponding to 2° and 4° of retinal eccentricities were automatically detected using built-in software (AO detect Mosaic b13; Imagine Eyes, France) in 50 $\mu\text{m} \times 50 \mu\text{m}$ zones. The analysis included the cone density, interphotoreceptor distance (average value of distances to neighboring cones), and packing regularity (number of nearest neighboring cones). For comparison, the same parameters were calculated in the corresponding areas of one eye of normal subjects.

Statistical Analysis

Descriptive data are presented as the mean \pm SD for quantitative variables and as counts and percentages for categorical variables. Comparisons between variables were performed using the Mann–Whitney test or

Table 1. Clinical and Imaging Data in the Asymptomatic Fellow Eyes of Patients With Unilateral Central Serous Chorioretinopathy Included in this Study

Age, Mean \pm SD, years	48.9 \pm 9.8
Gender, male, n (%)	14 (82.4%)
Previous corticosteroid intake*, n (%)	5 (35.7%)
BCVA of the asymptomatic fellow eye, logMAR, mean \pm SD (Snellen)	0 \pm 0 (20/20)
Clinical form of CSCR in the active eye	
Acute/recurrent, n (%)	7 (41.2%)
Chronic, n (%)	10 (58.8%)
Imaging of the asymptomatic fellow eyes	
OCT	
Extramacular pigment epithelium detachment and/or bulges outside the macular	11 (64.7%)
RPE bulge/irregularity, n (%)	4 (23.5%)
Pigment epithelium detachment, n (%)	7 (41.2%)
Macular photoreceptor line integrity	
Intact external limiting membrane, n (%)	17 (100%)
Intact ellipsoid zone, n (%)	17 (100%)
Subfoveal choroidal thickness (μ m), mean \pm SD	421.7 \pm 117.2
Autofluorescence	
RPE changes outside the macular, n (%)	10 (58.8%)
Indocyanine green angiography†	
Pachyvessels, n (%)	5 (38.5%)
Hyperfluorescent area in the midphase, n (%)	7 (53.8%)

*Data available for 14 patients.

†Available for 13 patients.

Student's t-test when appropriate. Statistical analyses were performed using XLSTAT software, version 2014.6.01 (Addinsoft, Paris, France). A *P*-value <0.05 was considered significant.

Results

Patient Characteristics

Seventeen patients with unilateral CSCR were included in this study. Patient characteristics are summarized in Table 1. The patient mean age was 48.9 \pm 9.8 years. Fourteen patients (82.4%) were male. A previous steroid use was reported in 5 of the 14 patients (35.7%) for whom these data were available. Seven patients (41.2%) had an acute/recurrent form of unilateral CSCR, and 10 patients (58.8%) had a chronic form of the disease. The mean BCVA was 0 \pm 0 logMAR (Snellen, 20/20). The subfoveal choroidal thickness was increased in the active CSCR eyes compared with the asymptomatic

fellow eye (453.3 \pm 101.8 μ m vs. 421.8 \pm 117.2 μ m; *P* = 0.05). In the asymptomatic fellow eyes, spectral domain-optical coherence tomography showed extramacular PED or bulges in 11 eyes (64.7%) and the foveal external limiting membrane and ellipsoid zone were continuous in all eyes on spectral domain-optical coherence tomography. In the asymptomatic fellow eyes, RPE changes outside the macular were observed in 10 eyes (58.8%) on BAF. Indocyanine green angiography, available in 13 asymptomatic fellow eyes, showed pachyvessels in the early phase in five eyes (38.5%) and hyperfluorescent plaques in the midphase in seven eyes (53.8%).

Comparison of Cone Density Between Asymptomatic Fellow Eyes of Patients With Unilateral CSCR and Control Subjects

The age-matched and gender-matched healthy control group consisted of 17 eyes of 17 subjects (Table 2). Adaptive optics fundus imaging showed a significant decrease in cone density at 2° of eccentricity nasal and temporal to the fovea in the asymptomatic fellow eyes of patients with unilateral CSCR compared with control subjects (*P* = 0.001 and *P* = 0.027, respectively). No statistically significant difference in cone density was found at 4° of eccentricity nasal and temporal to the fovea between both groups. In addition, the spacing of cones was higher at 2° of eccentricity nasal and temporal to the fovea in the asymptomatic fellow eyes of patients with unilateral CSCR compared with control subjects (*P* <0.001 and *P* = 0.04, respectively). No statistically significant difference in cone spacing was found at 4° of eccentricity nasal and temporal to the fovea between both groups.

Comparison of Cone Density of Asymptomatic Fellow Eyes of Patients With Unilateral Active CSCR According to the Clinical and Multimodal Imaging Findings

No statistically significant difference in cone density was found according to the previous corticosteroid intake, clinical form of CSCR in the active eye, presence of extramacular PED/bulges, subfoveal choroidal thickness, and presence of pachyvessels or hyperfluorescent area in the midphase of indocyanine green angiography (data not shown).

Discussion

We analyzed the cone density in asymptomatic fellow eyes of patients with unilateral CSCR using a commercial AO device. To avoid artifacts with AO,

Table 2. Cone Density and Spacing in the Asymptomatic Fellow Eyes of Patients With Unilateral Central Serous Chorioretinopathy (CSCR) Compared With the Control Group

	Asymptomatic Fellow Eyes of Patients with Unilateral CSCR (n = 17)	Control Subjects (n = 17)	P
Age, mean ± SD, years	48.9 ± 9.8	49.2 ± 7.1	0.9
Gender, male, n (%)	14 (82.4%)	14 (82.4%)	1
Cone density (cones/mm ²)			
2° of eccentricity nasal	25,468 ± 3,981	30,119 ± 3,083	0.001
4° of eccentricity nasal	19,941 ± 2,393	20,557 ± 1,216	0.38
2° of eccentricity temporal	25,802 ± 3,050	29,314 ± 5,439	0.027
4° of eccentricity temporal	20,484 ± 2,497	19,778 ± 2,142	0.4
Spacing (μm)			
2° of eccentricity nasal	7 ± 0.7	6.3 ± 0.3	< 0.001
4° of eccentricity nasal	7.9 ± 0.5	7.7 ± 0.3	0.22
2° of eccentricity temporal	6.9 ± 0.5	6.5 ± 0.7	0.04
4° of eccentricity temporal	7.8 ± 0.5	7.8 ± 0.4	0.4

asymptomatic fellow eyes with signs of previous subretinal detachment or PED in the macular area were excluded. The subfoveal choroidal thickness in the asymptomatic eyes was lower than that in the active CSCR eyes as previously reported¹⁶ and still above normative values.¹⁶ Signs of extramacular PPE were observed using OCT in 64.7% of asymptomatic fellow eyes. This rate is slightly higher than that previously reported⁶ but depends on the imaging modality used. Indeed, Ersoz et al⁵ have observed signs of PPE in 44.5% of asymptomatic fellow eyes using FA and in 61% of cases using multimodal imaging. In a previous study conducted in 68 patients with unilateral CSCR, we have found signs of PPE in 52% of asymptomatic fellow eyes using BAF, a rate consistent with the 58.8% of RPE changes observed on BAF in this study.⁶

The high frequency of RPE abnormalities in the asymptomatic fellow eyes of patients with CSCR suggested that a pathology affecting the choroid–RPE complex could precede the occurrence of a SRD, which is consistent with classical pathophysiological hypotheses. Indeed, we have previously shown that 19% of patients with PPE developed a subretinal detachment during a mean follow-up of 2 years.⁶ Another group has reported that 17% of patients with PPE developed CSCR during a 3-year follow-up.⁵ Some authors have assumed that PPE and CSCR could represent two stages of the same process caused by choroidal dysfunction.³

In CSCR, several studies have shown that a sustained subretinal detachment could cause photoreceptor damage and an irreversible vision loss.¹⁷ Current CSCR treatments with laser or photodynamic therapy aim to reduce the duration of the subretinal fluid.¹⁸ It remains to be determined whether other

mechanisms independent of the subretinal fluid could lead to photoreceptor damage. Our study showed a reduction in the number of juxtafoveal cones in the central 2° eccentricity, in the region where the blue cones density peaks (from 0.75 to 1.5°).¹⁹ Blue cones are first lost in several retinal diseases because of their increased sensitivity to oxidative stress.²⁰ In CSCR, this new finding could indicate an external neuroretinal suffering in the absence of any SRD in eyes with PPE.

This reduction could be due to not only an abnormal blood flow regulation in eyes with pachychoroid but also an excessive susceptibility to oxidative stress in patients with CSCR. Indeed, several articles have reported abnormal autonomous nervous system regulations in patients with CSCR^{21,22} and potentially an overperfusion of the outer retina with a subsequent higher risk of oxidative stress.²³ A recent work published by our group and others has identified systemic markers that could indicate an increased susceptibility to oxidative stress in patients with CSCR.²⁴ The level of lipocalin 2, a small acute stress protein involved in iron homeostasis that has been shown to play a crucial role in photooxidative-induced retinal damage in a rodent model,²⁵ is significantly reduced in the serum of patients with acute or chronic CSCR.²⁴ In addition, increased levels of oxidative stress biomarkers have been measured in patients with CSCR.^{26,27}

Our study has some limitations including its small sample size and the lack of follow-up. The choroidal thickness was not evaluated in our healthy control group. The AOSLO quantification with automated image analysis to count the cones could have slightly underestimated the cone density by 0% to 9% compared with a manual measurement.^{12,28,29} However, a manual measurement could also lead to misidentify rods as cones.³⁰

In conclusion, using AO, we found a significantly reduced cone density in the macula of asymptomatic fellow eyes of patients with unilateral CSCR. This result completes previous observations made with other imaging systems, showing that the external retina can be damaged independently of the occurrence of a SRD and is not solely a consequence of it. This could occur as a result of an abnormal choroidal flow regulation, mechanical stresses related to the pachyvessels, and an increased systemic susceptibility to oxidative stress. Further studies are needed to confirm this assumption.

Key words: central serous chorioretinopathy, pachychoroid, adaptive optics, optical coherence tomography.

Acknowledgments

The authors thank Marine Durand (Imagine Eyes, Orsay, France) for fruitful discussions.

References

- Daruich A, Matet A, Dirani A, et al. Central serous chorioretinopathy: recent findings and new physiopathology hypothesis. *Prog Retin Eye Res* 2015;48:82–118.
- Cheung CMG, Lee WK, Koizumi H, et al. Pachychoroid disease. *Eye* 2019;11:14–33.
- Siedlecki J, Schworm B, Priglinger SG. The pachychoroid disease spectrum-and the need for a uniform classification system. *Ophthalmol Retina* 2019;3:1013–1015.
- Warrow DJ, Hoang QV, Freund KB. Pachychoroid pigment epitheliopathy. *Retina* 2013;33:1659–1672.
- Ersoz MG, Karacorlu M, Arf S, et al. Pachychoroid pigment epitheliopathy in fellow eyes of patients with unilateral central serous chorioretinopathy. *Br J Ophthalmol* 2018;102:473–478.
- Shinojima A, Mehanna C, Lavia CA, et al. Central serous chorioretinopathy: risk factors for serous retinal detachment in fellow eyes. *Br J Ophthalmol* 2019;104:852–856.
- Ersoz MG, Karacorlu M, Arf S, et al. Outer nuclear layer thinning IN pachychoroid pigment epitheliopathy. *Retina* 2018;38:957–961.
- Liang J, Williams DR, Miller DT. Supernormal vision and high-resolution retinal imaging through adaptive optics. *J Opt Soc Am A Opt Image Sci Vis* 1997;14:2884–2892.
- Ooto S, Hangai M, Sakamoto A, et al. High-resolution imaging of resolved central serous chorioretinopathy using adaptive optics scanning laser ophthalmoscopy. *Ophthalmology* 2010;117:1800–1802.e2.
- Nakamura T, Ueda-Consolvo T, Oiwake T, Hayashi A. Correlation between outer retinal layer thickness and cone density in patients with resolved central serous chorioretinopathy. *Graefes Arch Clin Exp Ophthalmol* 2016;254:2347–2354.
- Curcio CA, Sloan KR, Kalina RE, Hendrickson AE. Human photoreceptor topography. *J Comp Neurol* 1990;292:497–523.
- Jacob J, Paques M, Krivosic V, et al. Comparing parafoveal cone photoreceptor mosaic metrics in younger and older age groups using an adaptive optics retinal camera. *Ophthalmic Surg Lasers Imaging Retina* 2017;48:45–50.
- Zitová B, Flusser J. Image registration methods: a survey. *Image Vis Comput* 2003;21:977–1000.
- Kulcsár C, Besnerais GL, Ödlund E, Lévecq X. Robust processing of images sequences produced by an adaptive optics retinal camera. *Optical Soc Am* 2013;2013:OW3A.3.
- Bidaut Garnier M, Flores M, Debellemanière G, et al. Reliability of cone counts using an adaptive optics retinal camera: reliability of adaptive optics camera. *Clin Exp Ophthalmol* 2014;42:833–840.
- Chen G, Tzekov R, Li W, et al. Subfoveal choroidal thickness in central serous chorioretinopathy: a meta-analysis. *PLoS One* 2017;12:e0169152.
- Wang MSM, Sander B, Larsen M. Retinal atrophy in idiopathic central serous chorioretinopathy. *Am J Ophthalmol* 2002;133:787–793.
- van Rijssen TJ, van Dijk EHC, Yzer S, et al. Central serous chorioretinopathy: towards an evidence-based treatment guideline. *Prog Retin Eye Res* 2019;73:100770.
- de Monasterio FM, McCrane EP, Newlander JK, Schein SJ. Density profile of blue-sensitive cones along the horizontal meridian of macaque retina. *Invest Ophthalmol Vis Sci* 1985;26:289–302.
- Greenstein VC, Hood DC, Ritch R, et al. S (blue) cone pathway vulnerability in retinitis pigmentosa, diabetes and glaucoma. *Invest Ophthalmol Vis Sci* 1989;30:1732–1737.
- Penas S, Castro P, Pereira G, et al. Cerebral neurovascular coupling impairment in central serous chorioretinopathy. *Ophthalmic Res* 2020. doi: 10.1159/000509553.
- Takeshima K, Tanaka K, Mori R, et al. Central serous chorioretinopathy and heart rate variability analysis with a smartphone application. *Sci Rep* 2020;10:14949.
- Cardillo Piccolino F, Lupidi M, Cagini C, et al. Choroidal vascular reactivity in central serous chorioretinopathy. *Invest Ophthalmol Vis Sci* 2018;59:3897–3905.
- Matet A, Jaworski T, Bousquet E, et al. Lipocalin 2 as a potential systemic biomarker for central serous chorioretinopathy. *Sci Rep* 2020;10:20175.
- Parmar T, Parmar VM, Perusek L, et al. Lipocalin 2 plays an important role in regulating inflammation in retinal degeneration. *J Immunol* 1950;200:3128–3141.
- Kunikata H, Sato R, Nishiguchi KM, Nakazawa T. Systemic oxidative stress level in patients with central serous chorioretinopathy. *Graefes Arch Clin Exp Ophthalmol* 2020;258:1575–1577.
- Turkoglu EB, Dikci S, Çelik E, et al. Thiol/disulfide homeostasis in patients with central serous chorioretinopathy. *Curr Eye Res* 2016;41:1489–1491.
- Garrioch R, Langlo C, Dubis AM, et al. Repeatability of in vivo parafoveal cone density and spacing measurements. *Optom Vis Sci* 2012;89:632–643.
- Talcott KE, Ratnam K, Sundquist SM, et al. Longitudinal study of cone photoreceptors during retinal degeneration and in response to ciliary neurotrophic factor treatment. *Invest Ophthalmol Vis Sci* 2011;52:2219–2226.
- Lombardo M, Serrao S, Ducoli P, Lombardo G. Eccentricity dependent changes of density, spacing and packing arrangement of parafoveal cones. *Ophthalmic Physiol Opt* 2013;33:516–526.